MAGNETIC SURVEYING AS AN AID TO GEOLOGICAL MAPPING: A CASE STUDY FROM OBAFEMI AWOLOWO UNIVERSITY CAMPUS IN ILE-IFE, SOUTHWEST NIGERIA

Oyeniyi, T. O., Salami, A. A. and Ojo, S.B.*

Department of Geology, Obafemi Awolowo University, Ile-Ife, Nigeria.

*Corresponding Author: sb_ojo@yahoo.com

(Received: 11th March, 2016; Accepted 28th April, 2016)

ABSTRACT

A magnetic map of the Obafemi Awolowo University (OAU) Campus, in Ile-Ife, was produced from ground magnetic measurements on all the roads and footpaths. The study was aimed at improving our knowledge of the structural disposition of the lithologies within the area. The magnetic data obtained were subjected to diurnal corrections, removal of the International Geomagnetic Reference Field, reduction to the magnetic equator, pseudogravity transformation and residualization to enhance the anomalies. The residual magnetic and pseudogravity anomaly maps were qualitatively and quantitatively interpreted using the total horizontal derivative, second vertical derivative, pseudogravity transformation, Euler deconvolution, and 2-D forward modeling techniques. The derivative maps showed that the area is clearly divided into three main magnetic (and pseudogravity) anomaly zones, demarcated by five contact locations (C1 to C5), which had close associations with the main lithologies of grey (or banded) gneiss, granite-gneiss and mica schist. The contact C1 indicated that the granite-gneiss might not be as extensive in the northwest as suggested by the geological map, while C4 and C5 indicated that the mica schist might in fact be less extensive, and the grey gneiss more extensive in the south. Two faults, F1 and F2, mapped by earlier workers in the north and south of the area respectively were centered along two broad quasi-linear NE-SW trending zones with relatively higher magnetic susceptibility and density than the host rocks. The faults were strike-slip faults, steeply dipping and could be associated with a zone of prominent magnetic low and pseudogravity high. The depth to the fault zones derived from Euler deconvolution solutions and forward modeling ranged from 18 to 40 m. The study concluded that the magnetic character of the two fault zones suggested zones of weakness in the upper crust through which more mafic rocks might have infiltrated.

Keywords: Ground magnetic, Pseudo-gravity, Subsurface Geology, Strike-slip Fault

INTRODUCTION

Background of Study

Geological and geophysical studies have been carried out by earlier workers to delineate the lithologies and map some major geologic structures in Obafemi Awolowo University Campus, North-West Ile-Ife (Boesse, 1989; Olorunfemi *et al.,* 1986; Ajayi and Adepelumi, 2001; and Fayemi, 2008). Geophysical mapping involves taking measurements at or near the Earth's surface to investigate the subsurface geology (Kearey *et al*., 2003). These measurements are influenced by the internal distribution of the physical properties of the subsurface lithologies and consequently, different lithologic units and geologic structures can be identified and located. However, the earlier geophysical studies of this area were based on a few isolated traverses and were thus limited in extent, hence the need for a more detailed survey.

The study area forms part of the Nigerian Basement Complex which contains an abundance of ferromagnesian minerals thus contributing to variations in the crustal component of the geomagnetic field. In the light of the existence of this physical property (magnetic susceptibility), this study adopted the ground magnetic method of geophysical prospecting in investigating the geologic structures in the study area at a low station-station spacing, averaging about 80 m.

Location and Characteristics of the Study Area

The study area is the Obafemi Awolowo University (OAU) Campus which lies in the north-western part of the town of Ile-Ife, Southwestern Nigeria (Fig. 1). It lies within the Universal Transverse Mercator (UTM) Zone 31N coordinate Y (828400 mN, 835600 mN) and X (666800 mE, 670800 mE) (Fig. 2), and the total survey area is approximately 30 km^2.

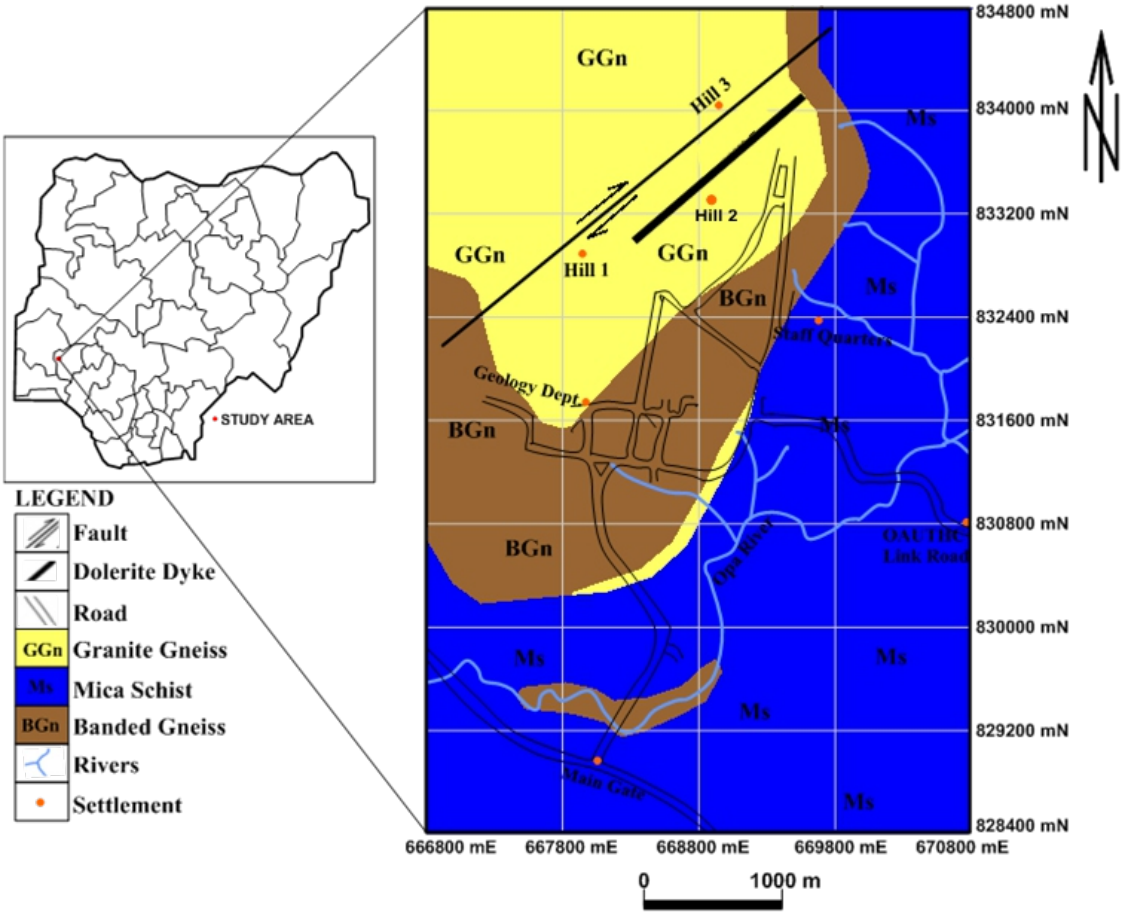

Figure 1. Geologic map of the Obafemi Awolowo University Campus (modified from Boesse, 1989).

Obafemi Awolowo University Campus can be classified as a magnetically noisy area consisting of buildings and car parks; and a magnetically quiet zone of low built-up areas. The area is accessible through the main gate in the southernmost part of the Campus when coming from either Ife-Ede road or Ife-Ibadan express road (Fig. 1), and also through the Obafemi Awolowo University Teaching Hospital Complex (OAUTHC) Link Road.

Physiography, Geomorphology, Geology, Drainage, Climate and Vegetation of the Study Area

The study area has a gently undulating topography in the southern part and a steeply undulating topography in the northern part (Fig. 2). The topographic elevation ranges from 200 metres to about 500 metres above sea level. The terrain consists of three gently rolling hills (Hill One, Hill Two and Hill Three in the NW) separated by swamps, boulder fields and small lakes. The hills, ridges, lakes and streams are generally elongated in a north-easterly direction following the bedrock structural grain. The main rock types that underlie the area are banded gneiss, mica schist and granite-gneiss (Boesse, 1989). The drainage pattern within the study area is dendritic (Fig. 1). The main river is the Opa River which flows northeastwards following the bedrock structural grain. There are two distinct seasons in the study area; the rainy season and the dry season. The rainy season is characterized by high rainfall between April and October with a mean annual rainfall of about 1237 mm (Bayowa *et al.,* 2011). The dry season which runs from November to March is characterized by dry dust originating from the Sahara Desert with occasionally low rainfall. Average temperature reaches a peak of 28.8°C in February and about 24.5°C in August (Bayowa *et al.,* 2011). The campus falls within the rain forest region of Nigeria. The vegetation comprises of herbs, grasses and light forest, most of which are evergreen. Such trees are common along the major roads within the campus.

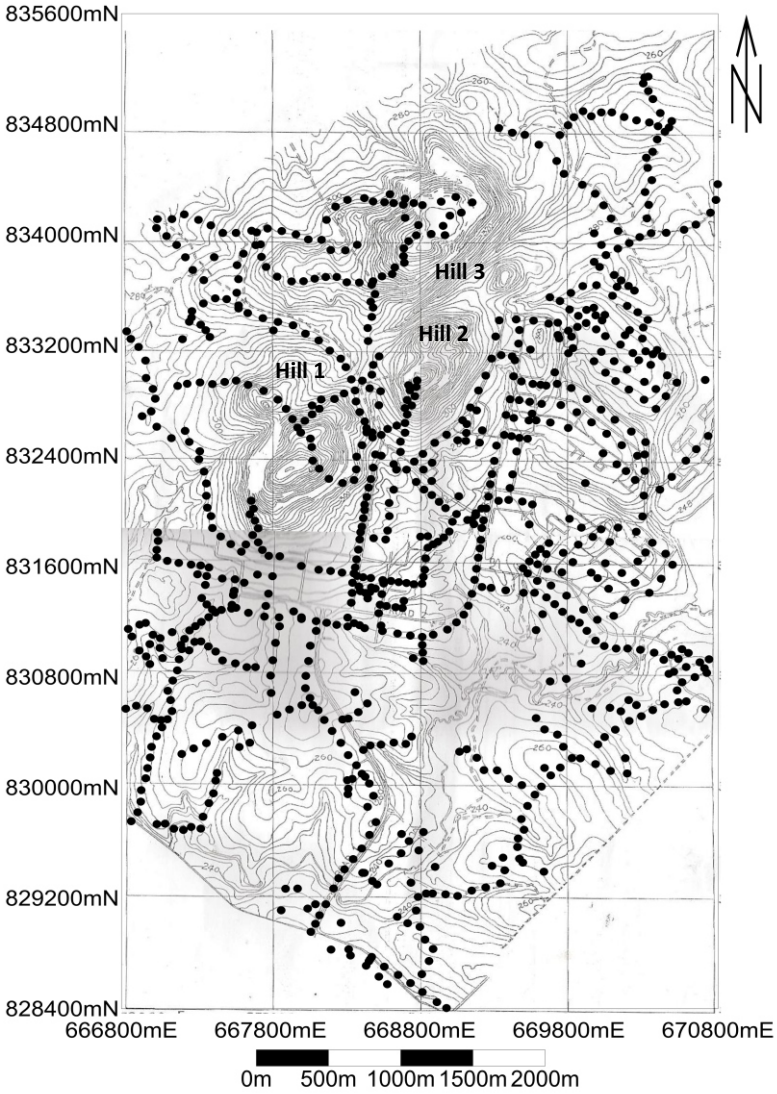

Figure 2.: The base map superimposed on the topographic map of the Campus, showing the distribution of the magnetic stations, and the major landmarks Hills 1, 2, and 3.

MATERIALS AND METHODS

Data Acquisition, Processing and Presentation

The magnetic data used for this study are ground magnetic data acquired between the months of March and April, 2014. The magnetometer used is one of the advanced GSM 19T series magnetometers – version 7 designed by GEM Systems belonging to the Geophysics Group of Department of Physics and Engineering Physics of OAU. It has a sensitivity of less than 0.1 nT, 0.01 resolution and 1 nT (+/- 0.5 nT) absolute accuracy over its full temperature range (GEM Systems, 2008). A network of 30 base stations (with one master base station) was established before magnetic readings were taken on all roads and footpaths at stations with an average station-station spacing of approximately 80 m (Fig. 2).

Diurnal correction, base level ties, removal of the International Geomagnetic Reference Field (IGRF) at each station, and noise filtering (by upward continuing the data to an elevation of 100 m) were carried out on the acquired data to increase the signal-to-noise ratio. The inclination and declination angles of the ambient field in the study area are -10.8° and -2.12°, respectively (at 831774 mN, 668879 mE) at the center of the study area, and an IGRF value of 33092.1 nT was subtracted from all the station readings. The reduction to equator (RTE) filter and pseudo-gravity filter were applied separately to the

magnetic data with the Geosoft package software, Oasis montaj™ v.6.4.2. The RTE filter removes the asymmetry associated with low latitude anomalies while the pseudo-gravity filter transforms the magnetic field into a pseudo-gravity field. Finally, residualization was carried out on the Total Magnetic Field Intensity (TMI) data and the Pseudo-gravity (PGA) data by removing the effect of the deep seated sources (regional) obtained by upward continuation of the maps to 1000 m.

Data Enhancement Techniques

The basic concepts of the magnetic method have been adequately explained in many geophysics text books (e.g. Blakely, 1996; Kearey *et al.*, 2003). After carrying out all the relevant corrections on the collected data, the residual magnetic anomaly (RMA) data and the residual pseudo-gravity anomaly (RPGA) data were subjected to a suite of signal enhancement techniques including total horizontal derivative (THD), Second Vertical Derivative (SVD) and 3-D standard Euler deconvolution technique. The theory and attributes of the different techniques used are briefly discussed in sections below.

Total Horizontal Derivative (THD) Technique

The total horizontal derivative technique is the simplest approach to estimate contact locations of bodies at depths (Ndougsa-Mbarga *et al.*, 2012). The biggest advantage of this method is its low sensitivity to noise in the data because it only requires calculations of the two first-order horizontal derivatives of the field (Phillips, 2002). If F is the potential field then the total horizontal derivative (THD) is given by:

$$\mathrm{THD}(x,y) = \sqrt{\left(\frac{\partial F}{\partial x}\right)^2 + \left(\frac{\partial F}{\partial y}\right)^2} \qquad (1)$$

This function gives a peak anomaly above the contacts for gravity and RTP magnetic anomalies. However, in magnetic equatorial regions where inclination is less than 15° (like the study area), RTP is generally unstable and cannot be easily derived. A similar effect is seen when a magnetic field is Reduced-to-Equator (RTE) instead of to the pole, or transformed to a pseudogravity map. For these reasons, the THD technique was carried out on the RPGA as well as the RMA data. Crests in the horizontal gradient magnitude grid can be located by passing a small 3 by 3 window over the THD grid and searching for maxima (Blakeley and Simpson, 1986).

Pseudo-Gravity Transformation

The magnetic potential V and gravitational potential U caused by a uniformly dense and uniformly magnetized body are related by the Poisson's relation (Blakely, 1996) expressed as:

$$V = \frac{-C_m}{G}\frac{M}{\rho} g_m \qquad (2)$$

where M is the intensity of magnetization, G is the Universal Gravitational Constant, ρ is the density, **m** is the direction of magnetization, and g_m is the component of the gravity field in the direction of magnetization **m**. C_m is a proportionality constant used to adjust units and in SI units is equal to $\frac{\mu_0}{4\pi} = 10^{-7}$ H/m. In deriving Poisson's relation, it is assumed that M and ρ are constant. A pseudo-gravity anomaly, calculated from a measured magnetic field, can be compared directly with measurements of the gravity field and is particularly useful because gravity anomalies are in many ways easier to interpret and quantify than magnetic anomalies.

Second Vertical Derivative (SVD) Technique

Second vertical derivatives are a measure of curvature, and large curvatures are associated with shallow anomalies. Second vertical derivatives enhance near surface effects at the expense of deeper anomalies (Telford *et al.*, 1990). The second vertical derivative can be obtained from the horizontal derivatives (Eq. 4) because the gravity and magnetic fields satisfy Laplace's equation. Thus,

$$\frac{\partial^2 F}{\partial z^2} = -\left(\frac{\partial^2 F}{\partial x^2} + \frac{\partial^2 F}{\partial y^2}\right) \qquad (3)$$

where, F is the potential field (gravity or magnetic) while x, y and z are the directions of differentiation. The quantities 0 mGal/m^2 and 0 nT/m^2 give the location of edges of geological features for gravity data and magnetic data (RTP or RTE) respectively.

3-D Standard Euler Deconvolution Technique

This technique provides automatic estimates of source location and depth. Therefore, Euler deconvolution is both a boundary finder and depth estimation technique. Euler deconvolution is commonly employed in potential field data interpretation because it requires only a little prior knowledge about the source geometry, and more importantly, it requires no information about the magnetization vector in the case of magnetics (Thompson, 1982; Reid *et al.*, 1990). The standard 3-D Euler deconvolution was used in this study and is based on solving Euler's homogeneity equation (Eq. 4) (Reid *et al.*, 1990):

$$(x - x_0)\frac{\partial T}{\partial x} + (y - y_0)\frac{\partial T}{\partial y} + (z - z_0)\frac{\partial T}{\partial z} = \eta(\beta - T) \qquad (4)$$

Equation (4) can be re-written as:

$$x\frac{\partial T}{\partial x} + y\frac{\partial T}{\partial y} + z\frac{\partial T}{\partial z} + \eta T = x_0\frac{\partial T}{\partial x} + y_0\frac{\partial T}{\partial y} + z_0\frac{\partial T}{\partial z} + \eta\beta \qquad (5)$$

where β is the regional value of the potential field and (x_0, y_0, z_0) is the position of the source, which produces the total potential field T measured at (x, y, z). η is the so-called structural index. For each position of the moving window, an over-estimated system of linear equations is solved for the position and depth of the sources (Thompson, 1982; Reid *et al.*, 1990).

The most critical parameter in the Euler deconvolution is the structural index, η (Thompson, 1982). This is a homogeneity factor relating the potential field and its gradient components to the location of the source. By changing η, the geometry and depth of the potential field sources can be estimated. A poor choice of the structural index has been shown to cause a diffuse solution of source locations and serious biases in depth estimation (Thompson, 1982; Reid *et al.*, 1990).

2-D Geological Modelling of the Subsurface

Two-dimensional (2-D) geologic models of the subsurface were produced with GM-SYS, a modelling package on Geosoft software, Oasis montaj™, version 6.4.2. The method used for calculating the magnetic response is based on the methods of Talwani *et al.* (1959), Talwani and Heirtzler (1964) using the algorithms described in Wen and Bevis (1987).

RESULTS AND INTERPRETATION

Total Magnetic Intensity and Pseudo-gravity Maps

The Total Magnetic Intensity (TMI) anomaly data after reduction to the magnetic equator and the pseudo-gravity (PGA) anomaly are presented as colour-shaded relief maps placed side by side in Figure 3. The residual magnetic anomaly (RMA) and the residual pseudo-gravity (RPGA) data are also presented as colour-shaded relief maps placed side by side in Figure 4.

The RMA and RPGA anomaly maps (Fig. 4) reveal that the dominant magnetic and pseudo-gravity anomaly trends are both aligned prominently in the NE-SW direction. These anomalies correspond respectively to magnetic susceptibility and density contrasts between the various lithologies of the crystalline basement rocks in the study area.

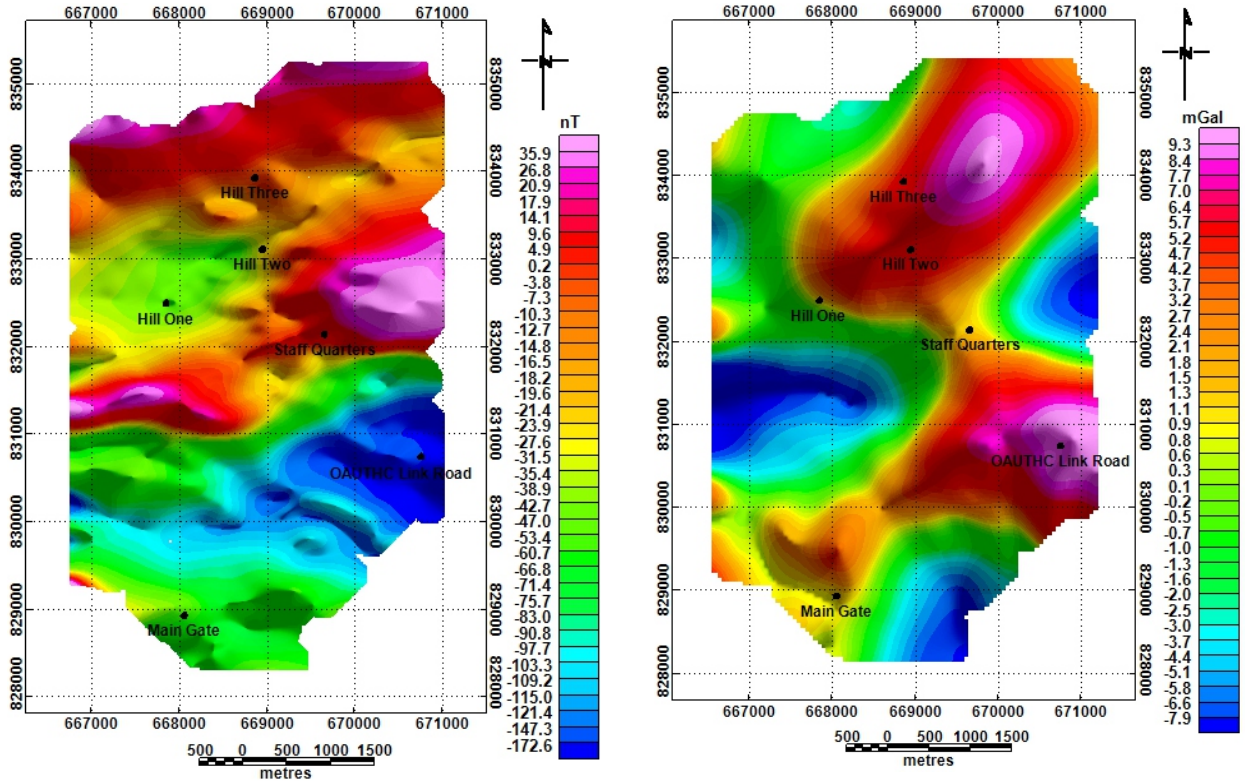

Figure 3 (a): Total magnetic field intensity (TMI) anomaly map of the OAU Campus after reduction to the Equator; (b) Pseudo-gravity (PGA) anomaly map of the Campus obtained from the TMI data.

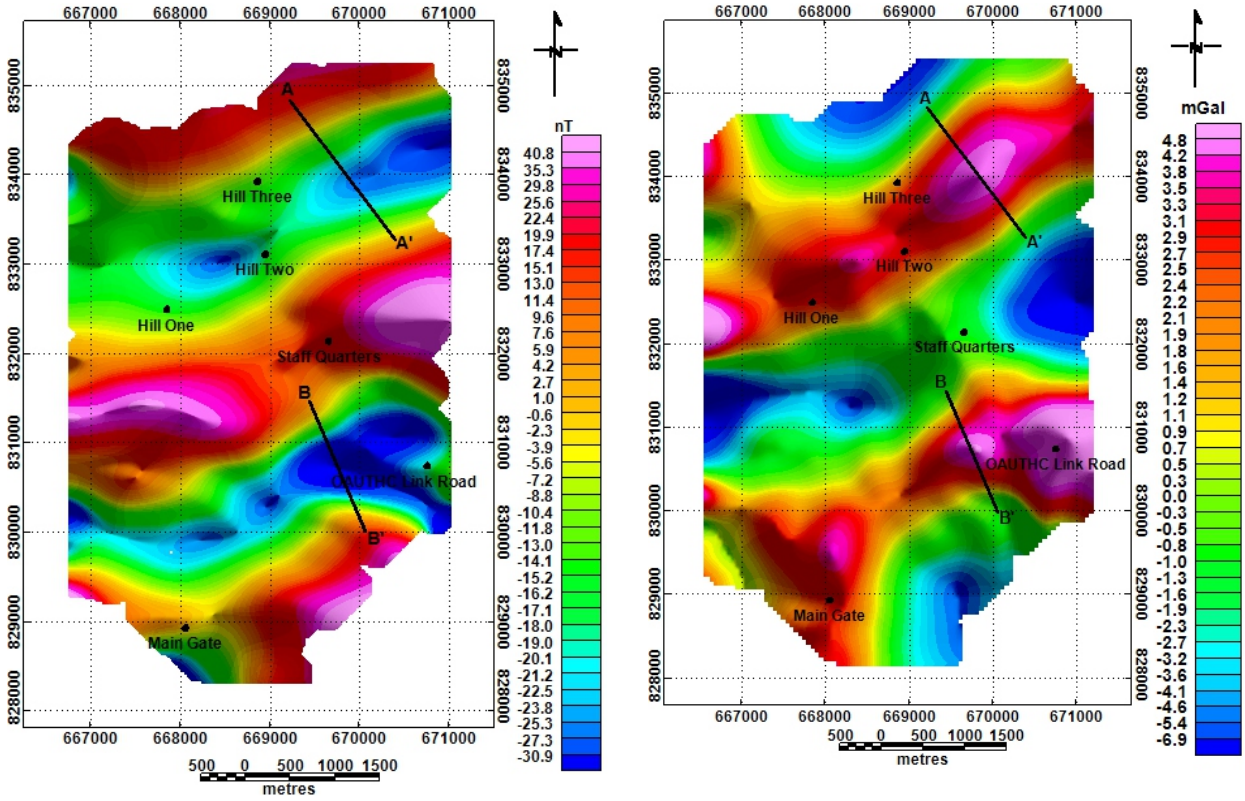

Figure 4 (a):Residual magnetic anomaly (RMA) map of the OAU Campus showing the 2-D model lines, A-A' and B-B'; (b) Residual pseudo-gravity (RPGA) anomaly map of the Campus showing the 2-D lines.

Areas of negative magnetic anomalies (corresponding at low magnetic latitudes to higher magnetic susceptibility) on the RMA map correspond to areas of high pseudo-gravity anomalies on the RPGA map (Fig. 4). The two maps (Fig. 4) show that the anomaly patterns in the northern and southern parts of the campus are essentially the same; low magnetic relief zones are encapsulated by high magnetic relief zones on the RMA map and high pseudo-gravity relief zones are encapsulated by low pseudo-gravity relief zones on the RPGA map (Fig. 4). The magnetic intensity of the RMA field ranges from -31 nT to 41 nT while the corresponding pseudo-gravity value on the RPGA field ranges from -7 mGal to +5 mGal.

Horizontal Derivative Maps

The results of the total horizontal derivative (THD) technique applied to the RMA and RPGA data are presented as colour-shaded relief maps overlain by the maxima of the THD in Figure 5. The THD results of the RMA and RPGA give contact locations that are continuous, thin and curvilinear (Fig. 5). The maps show major contacts in the ENE-WSW, NE-SW, E-W and NW-SE directions. The amplitudes of the gradient reach 0.085 nT/m on the RMA THD map and 0.014 mGal/m on the RPGA THD map. The contacts correspond to geological contact zones with a moderate magnetic susceptibility difference on the RMA THD map (Fig. 5a) and moderate density difference on the RPGA THD map (Fig. 5b). In order to highlight the contacts shown on the THD maps, the maxima of the THD maps were plotted as black lines on the THD maps (Fig. 5). The two THD maps show similar contact locations except in the southernmost part of the study area.

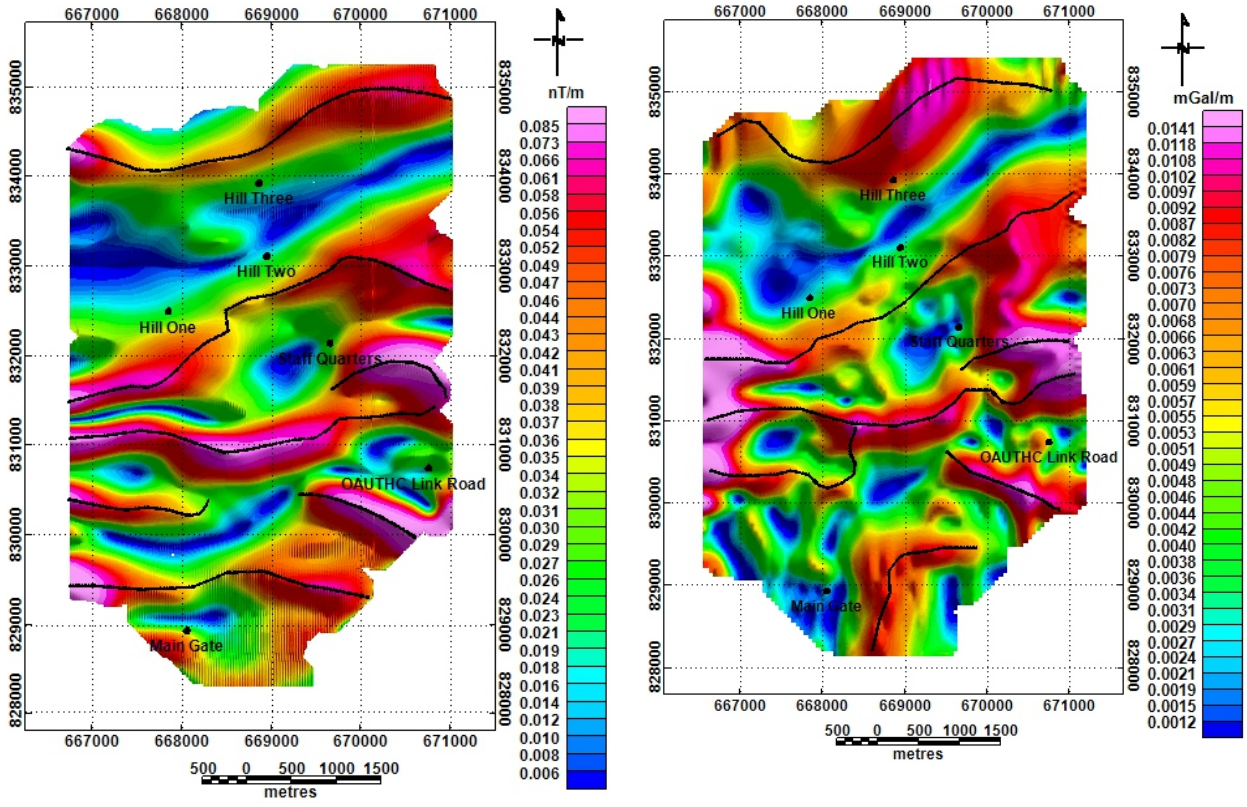

Figure 5: (a) THDR map of the RMA map showing the estimated locations of contacts as lines. (b)THDR map of the RPGA map showing the estimated locations of contacts as lines.

Second Vertical Derivative Maps

Similarly, the results of the second vertical derivative (SVD) analysis on the RMA and RPGA data are presented as colour-shaded relief maps overlain by the 0 nT/m^2 and 0 $mGal/m^2$ contour lines respectively in Figure 6.

The SVD technique does not usually result in displaced contacts because it does not require the assumptions in the THD technique. As a result of this, the final location of contacts are estimated using the following considerations; where the THD contacts are isolated or non-continuous, the SVD contact location gives the best contact location. In a similar manner, where the THD contacts are either parallel to or slightly offset from the SVD contact location, the SVD contact gives the preferred contact location. The SVD maps of the RMA and RPGA show similarities with their corresponding THD maps and the locations of contacts are indicated by 0 nT/m^2 contour lines on the RMA SVD map and 0 $mGal/m^2$ contour lines on the RPGA SVD map (Fig. 6). It is observed that the contact locations on the SVD maps also show better continuity than those on the THD maps.

Euler Deconvolution Analysis

The result of the analysis of 3-D Euler Deconvolution for the RMA data is presented as a colour-range symbol map in Figure 7. The technique determines the anomaly position, depth, and base level for a specific magnetic source. Several structural index values were tried for the Euler analysis and it was observed that a structural index of N = 0, representing a contact model, gave better clustering of the Euler solutions (Fig. 7).

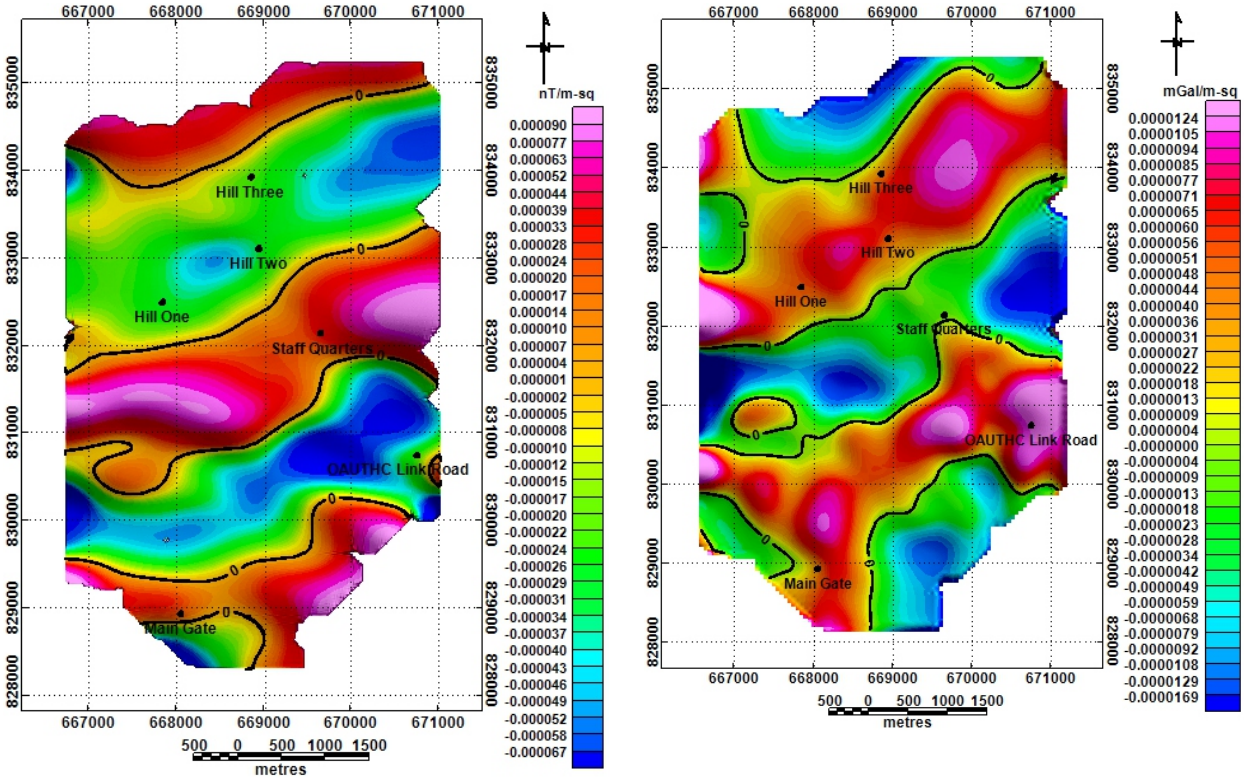

Figure 6: (a) SVD map of the RMA data overlain by the 0 nT/m^2 contour lines; (b) SVD map of the RPGA data overlain by the 0 $mGal/m^2$ contour line.

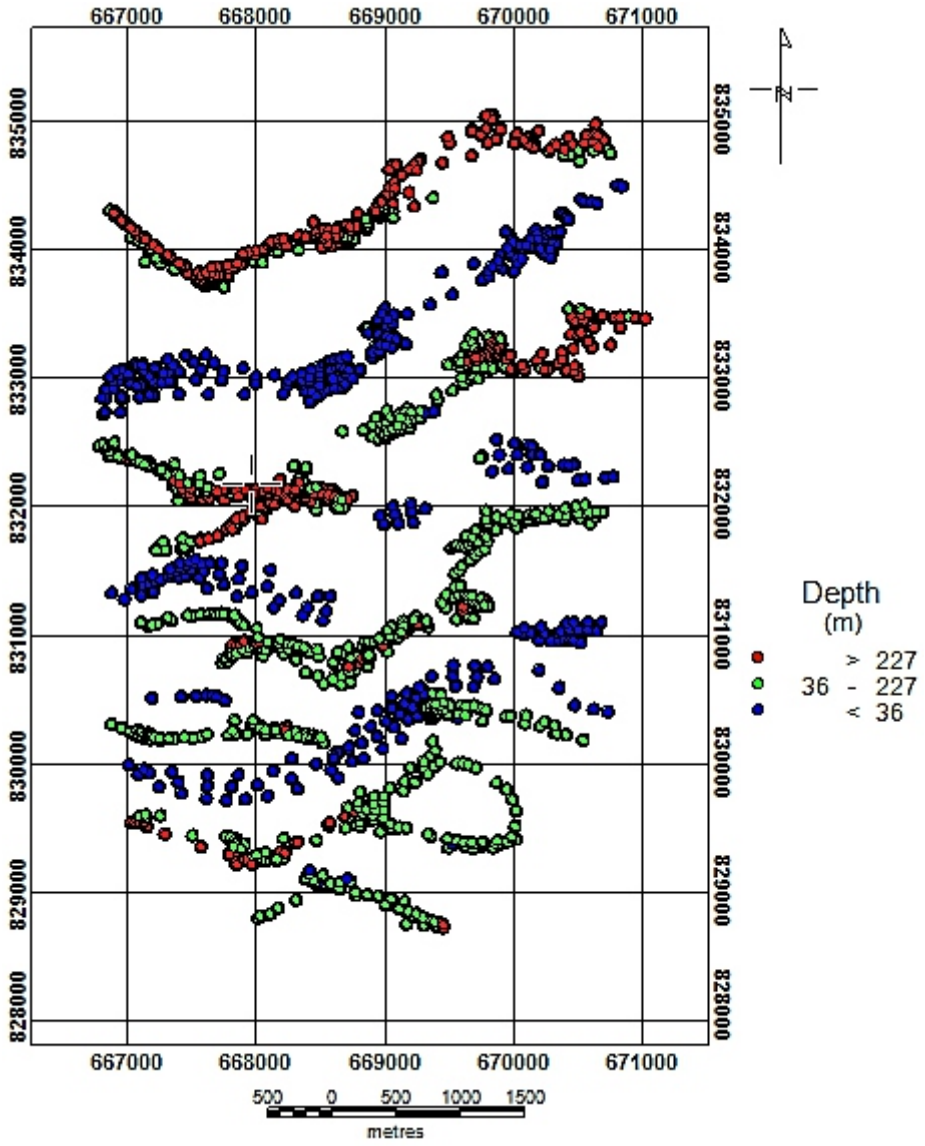

Figure 7: Map of Euler solutions for a structural index N=0.0, window size of 560 m × 560 m and maximum relative error of 40%. The solutions outline the lithological boundaries (red and green dots) and fault zones (blue dots).

The green and red points, which define solutions for depths that range from 36 to 227 m and greater than 227 m respectively, show the same consistent trends for the lithological contacts mapped by the THD and SVD results. The fault zone shown in the north of Figure 1 and mapped by Olorunfemi *et al.* (1986) is manifested as shallow blue coloured curvilinear points on the Euler map (Fig. 7). Another fault zone in the south (Olorunfemi and Okhue, 1992; Ajayi and Adepelumi, 2001; Kalejaiye, 2002) is similarly manifested as shallow blue-coloured curvilinear cluster of points in Figure 7. In the central region of Figure 7, further clusters of broken blue-coloured points suggest the presence of some minor faults not previously mapped. The uniform depth of solutions in the fault zones suggests that there is no vertical displacement and that the faults are most probably strike-slip in character.

2D Forward Modelling

The results of 2-D forward modelling carried out along two profiles, A - A' and B - B', taken on the RMA and RPGA (Fig. 4) are shown in Figure 8. The figures show similar results and revealed the depth to magnetic basement to be in the range of 9 to 85 m. The 2-D geologic models show the contacts to be near-vertical as suggested by the

Euler solutions and there is no vertical displacement on the cross sections in the fault zone supporting the suggestion that the faults are strike-slip in character.

DISCUSSION OF RESULTS

On the basis of the trends of the residual magnetic anomalies (Fig. 4a), the residual pseudo-gravity anomalies (Fig. 4b), the total horizontal derivative maps (Fig. 5), the second vertical derivative maps (Fig. 6), the Euler map (Fig. 7) and the main lithologies (Fig. 1), the study area is characterized by three main magnetic (and pseudo-gravity) anomaly zones demarcated by five contact locations (C1, C2, C3, C4 and C5) and two faults (F1 and F2).

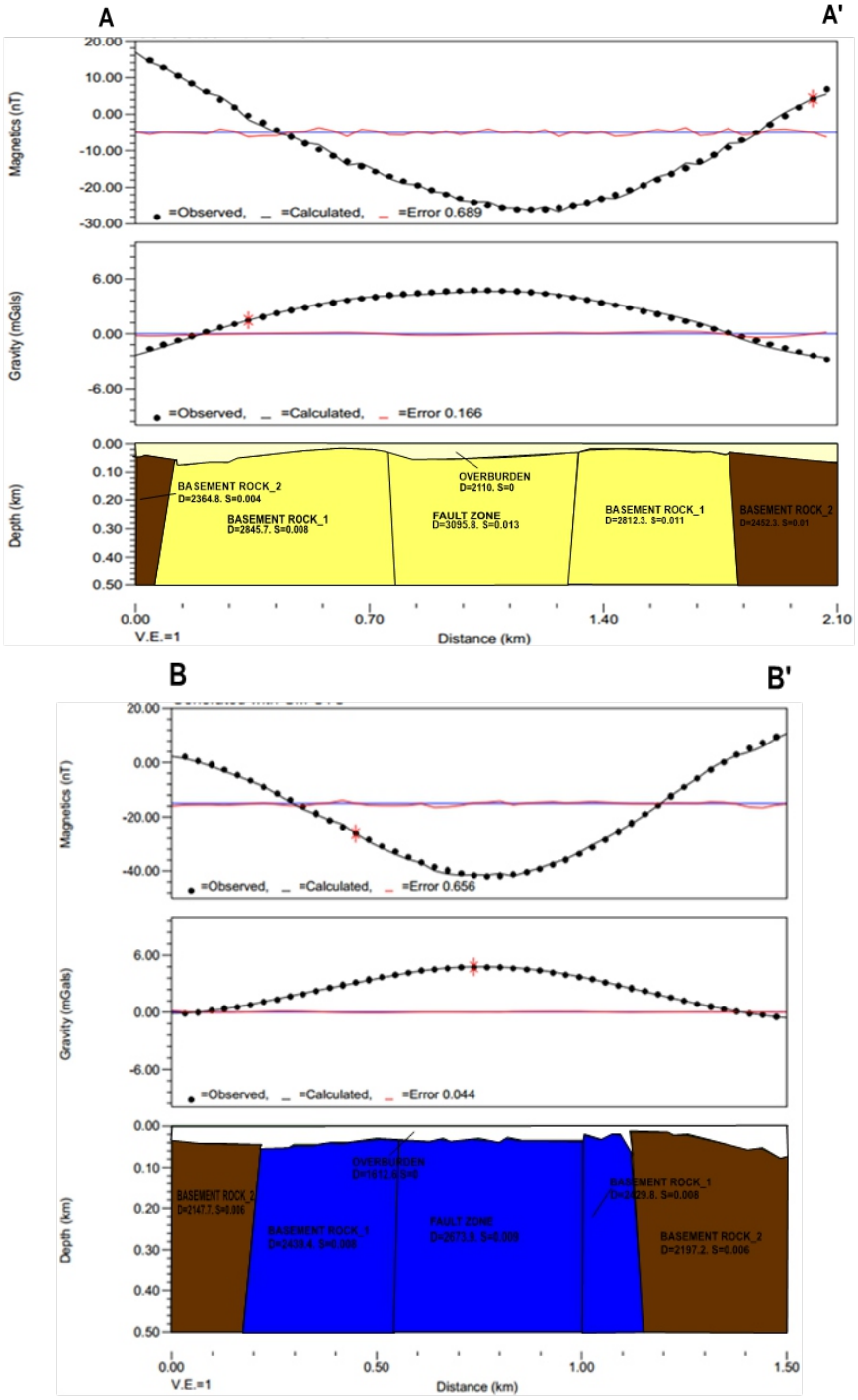

Figure 8: Geologic models of the subsurface obtained along (a) Profiles A-A' and (b) B-B' on the RMA and RPGA map.

Figure 9(a) shows these zones compared with the existing geological map (Fig. 9b). The zone between C1 and C2 (Fig. 9a) consists predominantly of granite-gneiss (Fig. 9b), while the zone between C3 and C4 (Fig. 9a) consists predominantly of mica schist. However, the granite-gneiss in the north-west of Figure 9(b) may not be as extensive as shown in the geological map (cf. Fig. 9a). In a similar manner, the lithology contacts C4 and C5 derived from the magnetic map (Fig. 9a) suggest that mica schist is not as extensive in the south and east of the area as indicated in Figure 9b; while the sliver of grey gneiss along Opa River (Fig. 9b) is probably more extensive (see Fig. 9a). The northern fault zone (F1) coincides with the zone of depression (low land) that separates Hill One and Hill Two from Hill Three (Fig. 9a). It has a strike of NE-SW, and its north-eastern segment coincides with a prominent dolerite dyke shown in Figure 9b. The fault cuts across a zone of relatively higher magnetic susceptibility and density. Its minimum depth of 21 m suggests that it lies beneath a thin cover of overburden. These results are consistent with the findings of Olorunfemi *et al.* (1986) and Fayemi (2008).

The southern fault zone (F2) coincides with the zone of depression which cuts across Road 1 and also trends in the NE-SW direction. It is a strike-slip fault in a zone characterized by relatively higher magnetic susceptibility and density. Its minimum depth of 22 m also indicates that it lies beneath a thin cover of overburden (see also Olorunfemi and Okhue, 1992; Ajayi and Adepelumi, 2001; and Kalejaiye, 2002). The magnetic character of dominant negative residual anomaly and positive pseudo-gravity anomaly, of the two major fault zones, suggest that they are zones of weakness in the upper crust through which more mafic rocks might have infiltrated.

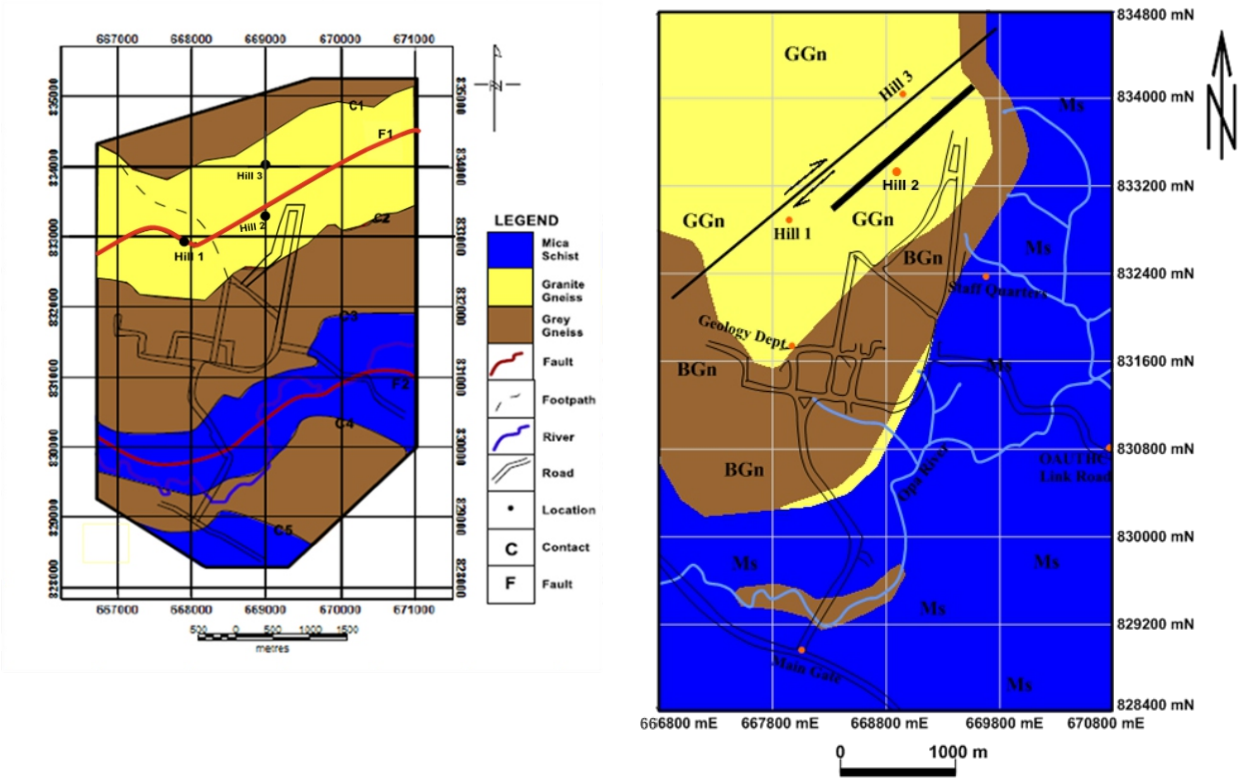

Figure 9. A comparison of the zonation map derived from the magnetic interpretation (left panel) with the geologic map of Boesse (1989) (right panel)

CONCLUSIONS

Ground magnetic investigation of OAU Campus, North-West Ile-Ife, was carried out with the aim of delineating the lithological units and the geologic structures in the area. Application of selected filtering methods to the magnetic data including reduction to the equator, horizontal and second vertical gradients, and pseudo-gravity transformation revealed three broad zones of NE-SW trending positive and negative residual magnetic and pseudo-gravity anomalies which could be roughly correlated with the lithology. Positive magnetic (or negative pseudo-gravity) residuals were associated with grey gneiss while negative magnetic (or positive pseudo-gravity) residuals were associated with granite-gneiss and mica schist. The maps clearly revealed two fault zones identified by earlier workers which trend in the NE-SW direction and cut across the zones of negative magnetic (or positive pseudo-gravity) residuals. The study concluded that the magnetic character of the two major fault zones suggested zones of weakness in the upper crust through which more mafic rocks might have infiltrated.

ACKNOWLEDGEMENTS

The authors are grateful to Dr. A. A. Adepelumi for some fieldwork supervision, Mr. F. Edino and Mr. A. Aderoju for assistance with aspects of the data processing, and Mr. O. B. Balogun for assistance with some of the figures. The support of the Geophysics Group of Department of Physics and Engineering Physics, Obafemi Awolowo University, Ile-Ife, in the form of the loan of a magnetometer is gratefully acknowledged.

REFERENCES

Ajayi, T. R. and Adepelumi, A. A. 2001. Reconnaissance soil-gas radon survey over the faulted crystalline area of Ile-Ife, Nigeria". *Env. Geology,* 41,608–613..

Bayowa, O. G., Ilufoye, D. T. and Animasaun, A. R. 2011. Geoelectric investigation of Awba earth dam embankment, University of Ibadan, Ibadan, Southwestern Nigeria, for anomalous seepages, *Ife Journal of Science*, 13, (2), 227-238.

Blakely, R. J. 1996. *Potential theory in gravity and magnetic applications*. Cambridge University Press, 441pp.

Blakely, R. J. and Simpson, R. W. 1986. Approximating edges of source bodies from magnetic or gravity anomalies. *Geophysics*, 51(7), 1494–1498.

Boesse, J. M. 1989. A Geological Map of the Obafemi Awolowo University Campus. *Unpublished B. Sc. Thesis*, Obafemi Awolowo University, Ile-Ife, Nigeria.

Fayemi, O. 2008. Geophysical characterization of the northern fault zone in Obafemi Awolowo University Campus. *Unpublished B. Sc. Thesis*, Obafemi Awolowo University, Ile-Ife, Nigeria, 75pp.

GEM Systems, 2008. GSM-19 v.7.0 Instruction Manual, 149pp.

Kalejaiye, H. O. 2002 Integrated geophysical survey of a fault zone over the southern part of Obafemi Awolowo University Campus. *Unpublished B. Sc. Thesis*, Obafemi Awolowo University, Ile-Ife, Nigeria.

Kearey, P., Brooks, M. and Hill, I. 2003. *An Introduction to Geophysical Exploration*, 3rd Edition. Blackwell Science.

Ndougsa-Mbarga, T., Feumoe, A. N. S., Manguelle-Dicoum, E. and Fairhead, J. D., 2012. Aeromagnetic Data Interpretation to Locate Buried Faults in South-East Cameroon. *Geophysica*, 48(1–2), 49–63.

Olorunfemi, M. O. and Okhue. 1992. Hydrogeologic and Geologic significance of a Geoelectric survey at Ile-Ife, Nigeria. *Journal of Mining and Geology*, 28(2), 221- 229.

Olorunfemi, M. O., Olarewaju, V. O. and Avci, M. 1986. Geophysical investigation of a fault zone – case history from Ile-Ife, southwestern Nigeria. *Geophysical Prospecting,* 34, 1277 – 1284.

Phillips, J. D. 2002. Processing and Interpretation of Aeromagnetic Data for the Santa Cruz Basin - Patahonia Mountains Area, South- Central Arizona. *U.S. Geological Survey Open-File Report*, 2002–2098.

Reid, A. B., Allsop, J. M., Granser, H., Millett, A. J. and Somerton, I. W. 1990. Magnetic interpretation in three dimensions using Euler deconvolution. *Geophysics*, 55, 80–90.

Talwani, M. 1965. Computation with the help of Magnetic Anomalies caused by arbitrary.

Geophysics, 30, 797–817.

Talwani, M. and Heirtzler, J. R. 1964. Computation of magnetic anomalies caused by two-dimensional bodies of arbitrary shape, in parks, G.A, Ed, *Computers in the mineral industries*, Part 1: Stanford Univer. Publ., Geological Sciences, 9, 464 - 480.

Telford, W. M., Geldart, L. P., Sheriff, R. E. and Keys, D. A. 1990. *Applied Geophysics*, 2nd Edition. Cambridge University Press.

Thompson, D. T. 1982. EULDPH: A new technique for making computer-assisted depth estimates from magnetic data. *Geophysics*, 47, 31–37.

Wen, I. J., and Bevis, M. 1987. Computing the gravitational and magnetic anomalies due to a polygon: algorithms and Fortran subroutines. *Geophysics*, 52, 232 -238.